Hubbard Model in Infinite Dimensions: A Quantum Monte Carlo Study

M. Jarrell

Department of Physics, University of Cincinnati, Cincinnati, Ohio 45221

(Received 5 December 1991)

An essentially exact solution of the infinite-dimensional Hubbard model is made possible by a new self-consistent Monte Carlo procedure. Near half filling antiferromagnetism and a pseudogap in the single-particle density of states are found for sufficiently large values of the intrasite Coulomb interaction. At half filling the antiferromagnetic transition temperature obtains its largest value when the intrasite Coulomb interaction $U \approx 3$.

PACS numbers: 75.10.Jm, 71.10.+x, 75.10.Lp, 75.30.Kz

The Hubbard model of strongly correlated electronic systems has been an enduring problem in condensed matter physics. It is believed to properly describe some of the properties of transition-metal oxides, and possibly high-temperature superconductors. Despite the simplicity of the model, no exact solutions exist except in one dimension [1]. Recently, a new approach [2–4] based on a dimensional expansion has been proposed to study such strongly correlated lattice models. In this paper, I present the first essentially exact numerical solution of the Hubbard model in the infinite-dimensional limit. This solution retains the physics expected in the low-dimensional model, including antiferromagnetism (Figs. 3, 4, and 5) and the formation of a correlation induced Mott-Hubbard gap in the single-particle density of states (Fig. 6).

The Hamiltonian of interest is

$$\mathcal{H} = -t \sum_{\langle ij\rangle,\sigma} (C^{\dagger}_{i,\sigma} C_{j,\sigma} + C^{\dagger}_{j,\sigma} C_{i,\sigma}) + \sum_i [\epsilon(n_{i,\uparrow} + n_{i,\downarrow}) + U(n_{i,\uparrow} - \tfrac{1}{2})(n_{i,\downarrow} - \tfrac{1}{2})] , \qquad (1)$$

where $C_{i,\sigma}$ ($C^{\dagger}_{i,\sigma}$) creates (destroys) an electron of spin σ on site i, and $n_{i,\sigma} = C^{\dagger}_{i,\sigma} C_{i,\sigma}$. This Hamiltonian will be studied in a hypercubic lattice dimension d in the limit as $d \to \infty$. The limit is taken subject to the constraint $4dt^2 = 1$, which yields a Gaussian unperturbed density of states, $\rho(\omega) = \exp(-\omega^2)/\sqrt{\pi}$ [2,3]. This is the only nontrivial way to take the limit, and is also appropriate for studying the magnetic properties of the model since the magnetic exchange $J \sim t^2/U$ multiplied by the number of neighbors is then kept fixed.

This limit greatly simplifies the problem. As shown in [3,4], this limit reduces the problem to a local problem since the nonlocal (intersite) dynamical interactions are negligible in this limit. Thus, the irreducible self-energy and irreducible vertex function are purely local, or site diagonal.

This fact may be seen from a diagrammatic argument [5]. Consider the first few diagrams of the single-particle self-energy for this problem as shown in Fig. 1. This is a real-space representation, so each electron propagator G_{ij} scales as $\sim t^{|\mathbf{R}_i - \mathbf{R}_j|}$. Thus the second-order term in Fig. 1 scales as $t^{3|\mathbf{R}_i - \mathbf{R}_j|}$. Consider the case where sites i and j are nearest neighbors, then even after summing over the contribution of a nearest-neighbor shell, the contribution of the second-order diagram is dt^3. This contribution vanishes in the limit as $d \to \infty$ since dt^2 is kept fixed when the limit is evaluated. A similar argument may be applied to all terms, and only the site-diagonal self-energy survives when the limit is evaluated. Furthermore, since the lattice is translationally invariant $\Sigma_{ij}(i\omega_n) = \Sigma(i\omega_n)\delta_{ij}$ independent of i. Thus, the solution of the single-particle properties reduces to solving $G_{ij}(i\omega_n) = G^0_{ij}(i\omega_n) + \sum_k G^0_{ik}(i\omega_n)\Sigma(i\omega_n)G_{kj}(i\omega_n)$ and the diagrammatic equation for Σ in Fig. 1 self-consistently.

With appropriate modifications, which I discuss below, these equations may be solved exactly with a self-consistent quantum Monte Carlo (QMC) scheme [6]. In the QMC part of the technique I introduce a local Green's function $\mathcal{G}$ on site i. The single-particle diagrams for $\mathcal{G}$ are illustrated in Fig. 2. Here, the undressed Green's function is the solution to the modified lattice

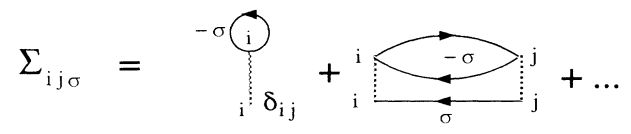

FIG. 1. The first few diagrams for the lattice self-energy. Here, the solid lines represent the undressed ($U=0$) electron propagators $G^0_{ij}(i\omega_n)$ and the dotted lines represent the intrasite interaction U.

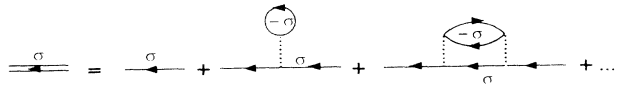

FIG. 2. The first few diagrams for $\mathcal{G}$ (double solid line) which is calculated in the QMC process. The undressed Green's function $\mathcal{G}^0$ is calculated from Eq. (2) and is represented here as a solid line, and the intrasite interaction U is represented as dotted lines.

problem:

$$\mathcal{G}^0(i\omega_n) = G'_{ii}(i\omega_n) = G^0_{ii}(i\omega_n) + \sum_k G^0_{ik}(i\omega_n)\Sigma'_k(i\omega_n)G'_{ki}(i\omega_n), \quad (2)$$

where

$$\Sigma'_k(i\omega_n) = \begin{cases} 0, & \text{if } i=k, \\ \Sigma(i\omega_n), & \text{otherwise.} \end{cases} \quad (3)$$

The prime indicates that the self-energy is set to zero on site i. This spatial dependence of Σ'_k is necessary to avoid overcounting of diagrams, since the Green's function $\mathcal{G}$ is calculated to all orders in U by the QMC process. The diagrammatic equation shown in Fig. 2 is the same as that needed to solve the Anderson impurity problem. Thus, given $\mathcal{G}^0$, I may solve for $\mathcal{G}$ with the QMC algorithm of Hirsch and Fye [7]. The Green's function calculated in this process may then be inverted to yield a new estimate for $\Sigma(i\omega_n)$,

$$\mathcal{G}(i\omega_n)^{-1} = \mathcal{G}^0(i\omega_n)^{-1} - \Sigma(i\omega_n). \quad (4)$$

Thus the QMC procedure and Eqs. (2) and (4) constitute a set of self-consistent equations for the lattice self-energy Σ which essentially reduce the problem to a self-consistently embedded Anderson impurity problem [8].

A variety of two-particle properties may also be calculated with this procedure [9], since, using similar arguments applied to the self-energy, one may argue that the irreducible vertex function is also local. For example, the static magnetic susceptibility matrix

$$\chi_{ij}(i\omega_n, i\omega_m) = \chi^0_{ij}(i\omega_n)\delta_{nm} + T\sum_{p,k}\chi^0_{ik}(i\omega_n)\Gamma(i\omega_n, i\omega_p) \times \chi_{kj}(i\omega_p, i\omega_m), \quad (5)$$

where $\omega_n = (2n+1)\pi T$. This is related to the static susceptibilities by

$$\chi_{\mathbf{q}} = \frac{T}{N}\sum_{n,m,i,j} e^{-i\mathbf{q}\cdot\mathbf{R}_{ij}}\chi_{ij}(i\omega_n, i\omega_m). \quad (6)$$

The noninteracting part is

$$\chi^0_{\mathbf{q}}(i\omega_n) = \frac{1}{N}\sum_{\mathbf{k}} G_{\mathbf{k}}(i\omega_n)G_{\mathbf{k}+\mathbf{q}}(i\omega_n), \quad (7)$$

where $G_{\mathbf{k}}(i\omega_n) = 1/[i\omega_n - \epsilon - \epsilon_{\mathbf{k}} - \Sigma(i\omega_n)]$. Equation (7) may readily be evaluated in the ferromagnetic [$\mathbf{q} = (0,0,0,\ldots)$] and antiferromagnetic [$\mathbf{q} = (\pi,\pi,\pi,\ldots)$] limits, in which it may be reexpressed as an integral over the Gaussian density of states. The function Γ is the local irreducible vertex function which may be calculated in the QMC procedure by solving

$$\chi_{ii}(i\omega_n, i\omega_m) = \mathcal{G}(i\omega_n)^2\delta_{nm} - T\sum_p \mathcal{G}(i\omega_n)^2\Gamma(i\omega_n, i\omega_p) \times \chi_{ii}(i\omega_p, i\omega_m). \quad (8)$$

Here χ_{ii} is the opposite-spin two-particle Green's function,

$$\chi_{ii}(i\omega_n, i\omega_m) = -T^2\int_0^\beta d\tau_1\int_0^\beta d\tau_2\int_0^\beta d\tau_3\int_0^\beta d\tau_4 e^{-i\omega_m(\tau_1-\tau_2)}e^{-i\omega_n(\tau_3-\tau_4)}\langle T_\tau C_{i,\uparrow}(\tau_4)C^\dagger_{i,\downarrow}(\tau_3)C_{i,\downarrow}(\tau_2)C^\dagger_{i,\uparrow}(\tau_1)\rangle \quad (9)$$

and $\mathcal{G}$ is the corresponding fully dressed single-particle Green's function.

Both $\mathcal{G}$ and χ_{ii} are calculated in the QMC procedure. Here the problem is cast into a discrete path formalism in imaginary time, τ_l, where $\tau_l = l\Delta\tau$, $\Delta\tau = \beta/L$, and L is the number of times slices. The values of L used ranged from 40 to 160, with the largest values of L reserved for the largest values of β since the time required by the algorithm scales like L^3. No "sign problem" was observed at any filling. At the start of the QMC process the initial Green's function (for which $U=0$ on the simulated site) is taken to be $\mathcal{G}^0$. The algorithm produces $\mathcal{G}$, which is used in Eqs. (4) and (2) to produce another estimate for Σ and $\mathcal{G}^0$. This process is continued until $\mathcal{G} = G_{ii}$ within the numerical precision of code. Usually five to eight iterations are required for convergence. Other quantities such as χ_{ii}, $\mu^2 = \langle(n_\uparrow - n_\downarrow)^2\rangle$, etc., are calculated on the last iteration, once convergence is reached.

It is expected that the Hubbard model will exhibit antiferromagnetism at half filling. This transition is signaled by the divergence of the antiferromagnetic susceptibility χ_{AF} calculated using the methods described above. Results from this approach are shown in Fig. 3 for $U=1.5$ and $\epsilon=0.0$. The logarithmic scaling behavior is shown in the inset. Near T_c the data fit a form $\chi_{AF} \propto |T-T_c|^\nu$ with $T_c = 0.866 \pm 0.0003$ and $\nu = -0.99 \pm 0.05$. This scaling behavior is consistent with that of a Heisenberg model on a lattice with an infinite number of nearest neighbors, for which one expects the Curie-Weiss mean-field form for χ_{AF}.

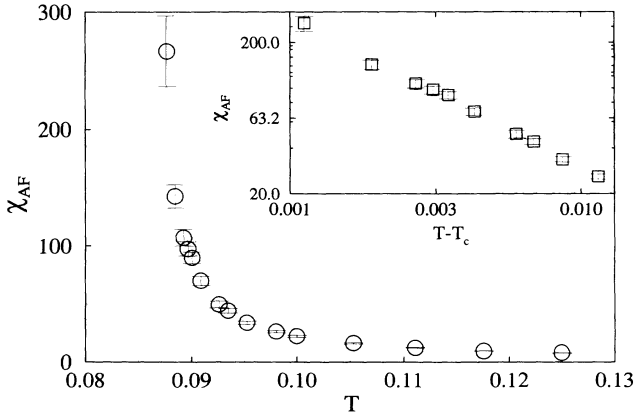

FIG. 3. Antiferromagnetic susceptibility $\chi_{AF}(T)$ vs temperature T when $U=1.5$ and $\epsilon=0.0$. The logarithmic scaling behavior is shown in the inset. The data close to the transition fit the form $\chi_{AF} \propto |T-T_c|^\nu$ with $T_c = 0.0866 \pm 0.0003$ and $\nu = -0.99 \pm 0.05$. The points at $U=0$ reflect exactly known limits.

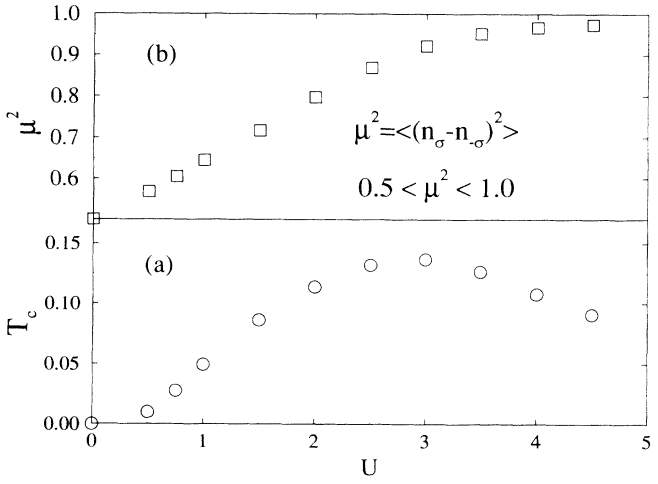

FIG. 4. (a) Antiferromagnetic T_c and (b) $\mu^2=\langle(n_\uparrow-n_\downarrow)^2\rangle$ (calculated at $T=T_c$) plotted vs U for the half-filled model ($\epsilon=0$). In each case, the error bars are smaller than the plotting symbols.

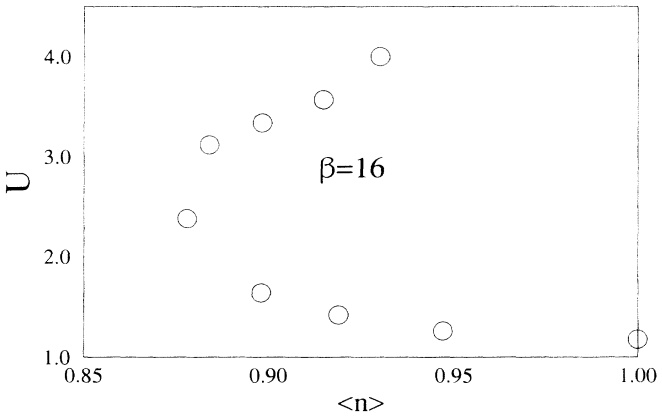

FIG. 5. Critical values of U, where χ_{AF} diverges, vs filling for fixed $\beta=16$. The result is symmetric around $\langle n\rangle=1$.

The antiferromagnetic transition temperature T_c for the half-filled model is plotted as a function of U in Fig. 4(a) [10]. For small values of U, where the local spin moment is also small, I find that T_c is exponentially small, consistent with perturbation theory [11]. For very large values of U, where the spin moment has saturated to its maximum value, one expects that the transition temperature will fall monotonically with increasing U, $T_c \sim 1/U$ [11]. This is because the antiferromagnetic exchange $dJ \sim dt^2/U$ also decreases with increasing U. Thus, one expects a peak in $T_c(U)$ for some intermediate value of U as seen in Fig. 4(a). In Fig. 4(b) the unscreened squared moment $\mu^2=\langle(n_\uparrow-n_\downarrow)^2\rangle$, calculated at the transition $T=T_c$, is plotted versus U when $\epsilon=0$. For the half-filled model μ^2 ranges from $\mu^2=0.5$ in the uncorrelated limit ($U=0$) to $\mu^2=1$ in the strongly correlated limit ($U\rightarrow\infty$). Note that the peak in $T_c(U)$ occurs near the point where μ^2 begins to saturate to one. Away from half filling, the divergence of the antiferromagnetic susceptibility is quickly suppressed. This behavior when $\beta=16$ is shown in Fig. 5 where the critical value of U is plotted versus filling.

The infinite-dimensional Hubbard model also appears to exhibit Mott-Hubbard behavior. This can be seen in the single-particle density of states $A(\omega)=-1/\pi \mathrm{Im} G_{ii}(\omega+i0^+)$ of the half-filled model as shown in Fig. 6. Here A is plotted for several values of U when $\beta=7.2$ and $\epsilon=0$. These results were produced by analytically continuing the imaginary time Green's function $G_{ii}(\tau)$ with the maximum entropy procedure [12–14]. The unperturbed density of states $\rho(\omega)=\exp(-\omega^2)/\sqrt{\pi}$ was taken as the default model in this procedure. As the Hubbard U is increased from zero, the spectrum begins to develop a pseudogap at zero frequency, whereas, away from half filling (not shown) this pseudogap disappears quickly. This feature is identified as a pseudogap, since, although exponentially small, the $\omega=0$ density of states can never go completely to zero in this model [15].

The method described in this paper has reduced the infinite-dimensional Hubbard model to a self-consistently embedded Anderson impurity problem. Thus for large U the qualitative features of the density of states have a possible interpretation in terms of the Anderson model spectrum. The upper and lower peaks correspond to charge transfer on and off the local site being simulated. The central peak may correspond to the Abrikosov-Suhl resonance, which indicates the formation of a quasiparticle which reduces the screened local moment on each lattice site.

In addition to noting what behavior was observed in the infinite-dimensional Hubbard model, it is worthwhile to note what behavior was not. For all fillings, temperatures, and correlations simulated, the ferromagnetic and

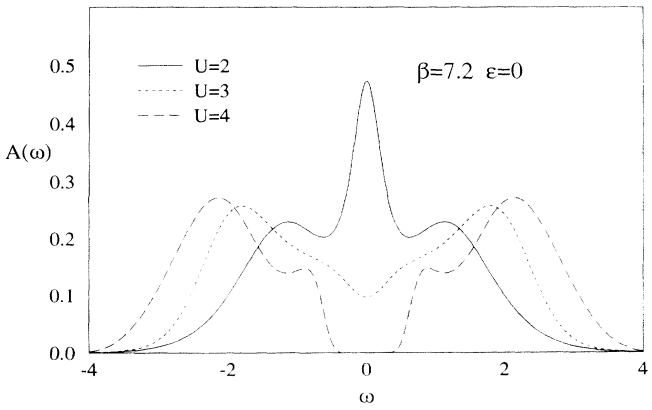

FIG. 6. Density of states $A(\omega)=-(1/\pi)\mathrm{Im}[G_{ii}(\omega+i0^+)]$ vs ω when $\epsilon=0.0$ and $\beta=7.2$ for various values of U. These results are for the paramagnetic state.

s-wave superconducting susceptibilities did not diverge.

In conclusion, I have presented a self-consistent quantum Monte Carlo procedure which allows one to simulate strongly correlated systems in the limit of infinite dimensions. I have shown that the model displays the expected antiferromagnetism when half filled, and that the single-particle density of states displays a correlation pseudogap. The importance of this result is that it allows an essentially exact solution of the $d=\infty$ Hubbard model in the thermodynamic limit. Thus, solutions now exist for the model in two limits, $d=1$ [1] and $d=\infty$. Finally, while this method is discussed in the context of the Hubbard model, it could be applied to other strongly correlated models (i.e., the periodic Anderson model) just by changing the form of the undressed Green's functions in Eqs. (2) and (5).

I would like to acknowledge useful conversations with D. L. Cox, J. Freericks, J. E. Gubernatis, M. Ma, F. J. Pinski, T. Pruschke, and R. Scalettar. This work was supported by the National Science Foundation Grant No. DMR-9107563 and by the Ohio Supercomputing Center.

[1] E. H. Lieb and F. Y. Wu, Phys. Rev. Lett. **20**, 1445 (1968).

[2] W. Metzner and D. Vollhardt, Phys. Rev. Lett. **62**, 324 (1989).

[3] E. Müller-Hartmann, Z. Phys. B **76**, 211 (1989); **74**, 507 (1989).

[4] P. G. J. van Dongen and D. Vollhardt, Phys. Rev. Lett. **65**, 1663 (1990).

[5] H. Schweitzer and G. Czycholl, Z. Phys. B **77**, 327 (1990).

[6] A similar self-consistent QMC procedure was used to treat magnetic impurities in a superconducting host. M. Jarrell, D. S. Sivia, and B. Patton, Phys. Rev. B **42**, 4804 (1990).

[7] J. E. Hirsch and R. M. Fye, Phys. Rev. Lett. **56**, 2521 (1986).

[8] Upon completion of this work, I obtained a copy of work by A. Georges and G. Kottliar [Phys. Rev. B **45**, 6479 (1992)] in which this connection with the Anderson impurity is also made, and perturbation theory in U is used to generate approximate results for $A(\omega)$.

[9] V. Zlatić and B. Horvatić (to be published).

[10] When properly scaled, $T_c(U)$ reported here for half filling is in remarkable agreement with results for the three-dimensional model reported in R. T. Scalettar *et al.*, Phys. Rev. B **39**, 4711 (1989).

[11] P. G. J. van Dongen, Phys. Rev. Lett. **67**, 757 (1991).

[12] J. E. Gubernatis *et al.*, Phys. Rev. B **44**, 6011 (1991).

[13] R. K. Bryan, Eur. Biophys. J. **18**, 165 (1990).

[14] R. N. Silver *et al.*, Phys. Rev. B **41**, 2380 (1989).

[15] W. Krauth (private communication); see also Ref. [8].